Detonation Physics-Based Modelling & Design of a Rotating Detonation Engine

Sean Francis Connolly-Boutin

A thesis
in
The Department
of
Mechanical, Industrial and Aerospace Engineering

Presented in Partial Fulfillment of the Requirements
For the Degree of
Master of Applied Science (Mechanical Engineering)
Concordia University
Montréal, Québec, Canada

January 2020

Concordia University
School of Graduate Studies

This is to certify that the thesis prepared

By: **Sean Francis Connolly-Boutin**

Entitled: **Detonation Physics-Based Modelling & Design of a Rotating Detonation Engine**

and submitted in partial fulfillment of the requirements for the degree of

Master of Applied Science (Mechanical Engineering)

complies with the regulations of this University and meets the accepted standards with respect to originality and quality.

Signed by the final examining commitee:

_____ Chair

Dr. Lyes Kadem

_____ Examiner

Dr. Rolf Wutrich

_____ Examiner

Dr. Hoi Dick Ng

_____ Supervisor

Dr. Charles Kiyanda

Approved _____

Dr. Waiz Ahmed, Chair of Department or Graduate Program Director

January 8, 2020 _____

Amir Asif, Ph.D.,P.Eng, Dean

Gina Cody School of Engineering and Computer Science

Abstract

Detonation Physics-Based Modelling & Design of a Rotating Detonation Engine

Sean Francis Connolly-Boutin

A rotating detonation engine (RDE) is a new, more thermodynamically efficient, propulsion concept that replaces the traditional constant pressure combustion mechanism found in all currently used rockets and power generation devices. The constant pressure combustion is replaced by a detonation wave: a coupled shock-flame complex propagating at speeds of up to 2-3 km/s and generating combustion products at pressures 5-10 times the initial reactant pressure. This pressure gain through the combustion process leads to more compact, simpler devices that no longer require (or depend less upon) initial reactant precompression. Detonation-based cycles also have the added advantage of being theoretically more thermodynamically efficient than their constant pressure combustion counterparts. As such, RDEs have become increasingly popular in the propulsion research community, although there is still a lack of understanding in the underlying physics which govern their operability, though the existence of a minimum mass flow rate limit for stable operation has been observed. To help engineers and researchers design an RDE, a model was developed which combines geometric properties, 1D isentropic flow, and detonation physics to predict the stable operating bounds of an RDE. An engine testing facility was also constructed in collaboration with McGill University to test RDEs and confirm the performance of the prediction model developed.

Acknowledgments

First and foremost, I must thank my advisor Prof. Charles Basenga Kiyanda for supporting my research and guiding me throughout this project. Next, I must thank Prof. Andrew Higgins of McGill University for allowing us to build a blowdown facility for engine tests in his laboratory at McGill, and for his input in the design and experimentation process which was invaluable to the advancement of the project. I must also give special thanks to my undergraduate Capstone Design Project team: Victoria Joseph, Susan Fahmy, Marc Alexandre Allard and Somyya Ahmed Butt. Their contributions proved invaluable in setting the groundwork for this degree, and as a testament to their contributions their names are still shown in much of the technical drawings for the engine as well as the technical reports which followed. Next, I'd like to thank my parents Michel Boutin and Jo-Ann Connolly who provided me with much needed emotional and financial support throughout my studies, and who taught me that perseverance when faced with difficult times tells you more about a person's abilities and determination than a few bad grades do. Without these lessons, I may never have even considered applying to graduate school. Finally, I would like to thank Café Myriade on MacKay Street for keeping me alert when I needed it most with their delicious coffee.

Contents

List of Symbols

D	Nominal Engine Diameter
h	Combustion Chamber Annulus Thickness
L_{cr}	Length of Detonating Zone in the Combustion Chamber
C	Proportionality Constant
C_L	Scaled Proportionality Constant
$\dot{m}$	Mass Flow Rate Through the Engine
P	Pressure
T	Temperature
U_{CJ}	Chapman-Jouguet Detonation Wave Speed
U_D	Detonation Wave Speed
V_{inj}	Velocity of Injected Reactants
θ	Angle of Reactant Injection Surface
λ	Detonation Cell Width
ρ	Density
R_s	Specific Gas Constant
ϕ	Equivalence Ratio
Y	Mass Fraction
M	Mach Number
γ	Ratio of Specific Heats
ω	Wavenumber: Number of Co-rotating Detonation Waves within the Combustion Chamber
$\%\Delta$	Percent Difference

$\{\}^*$	Choking Property
$\{\}_0$	Stagnation Property
$\{\}_{ref}$	Reference State
$\{\}_{inj}$	Injection Property
$\{\}_{cc}$	Combustion Chamber (Annulus) Property
$\{\}_i$	Property of Single Reactant
$\{\}_{mix}$	Reactant Mixture Property

List of Acronyms

CEA	Chemical Equilibrium with Applications
GALCIT	Graduate Aerospace Laboratories of the California Institute of Technology
JAXA	Japan Aerospace Exploration Agency
NASA	National Aeronautics and Space Administration
PDE	Pulse Detonation Engine
PGC	Pressure Gain Combustion
P&ID	Piping & Instrumentation Diagram
RDE	Rotating Detonation Engine

List of Figures

List of Tables

Chapter 1

Introduction

Over the last two decades, rotating detonation engines (RDEs) have been of particular interest to researchers in the fields of shock wave and detonation physics, and aerospace propulsion. As environmental regulations have become more strict, the need to develop more efficient combustion concepts has increased. Numerous concepts have been investigated, such as scramjet engines and pulse detonation engines (PDEs), though each of these have certain operability problems. PDEs operate cyclically, where the combustor must be filled with a fuel mixture, detonated, purged, and refilled with fresh unburned mixture before being reignited [1]. In other words, PDEs must be reignited with each new combustion cycle. Scramjets do not have this issue, however, they require a high-velocity flow field to be ignited in the first place. On the other hand, RDEs avoid both of these issues while maintaining the gain in efficiency that occurs with detonative cycles [2].

1.1 Basic Rotating Detonation Engine Operation

An RDE operates by sustaining a number of detonations travelling circumferentially around an annular combustor, as shown in fig. 1b. The detonations themselves are the primary means of energy extraction, and differ widely from the current commercially available combustion concepts. As opposed to combustion inside gas turbine or rocket engine combustors, which operate under a constant pressure thermodynamic process using a pre-compressed fuel mixture, detonations propagate as a combined supersonic shock and combustion complex.

1.2 Detonation Dynamics and Structure

In 1D geometry, detonation waves are composed of a supersonic moving shock wave, followed by a reaction zone and a sonic plane as shown in fig. 2. The presence of the sonic plane (or the limiting characteristic in multi-dimensions) is what defines the Champan-Jouguet solution of detonations. For a CJ wave, pertubations beyond the sonic plane do not affect the detonation structure. Detonations propagate at a natural, maximum velocity called the Chapman-Jouguet velocity, U_{CJ}, and generate a high pressure state, the CJ state, (P_{CJ},T_{CJ}). In two and three dimensions, the detonation structure

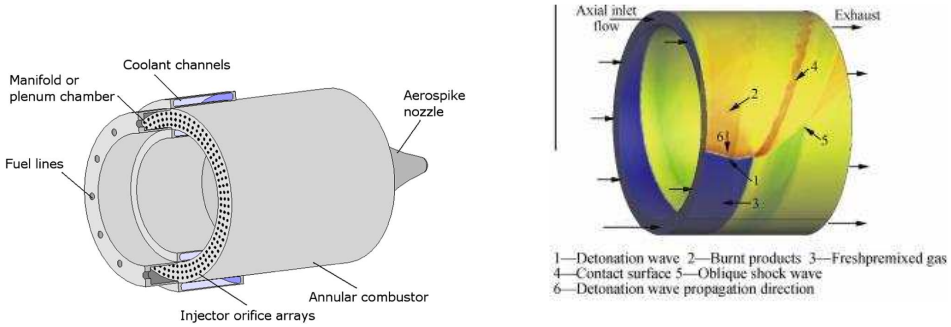

(a) Typical RDE Configuration [3]

(b) Typical RDE flow field for single wave operation [4]

Figure 1: RDE configuration and flow field

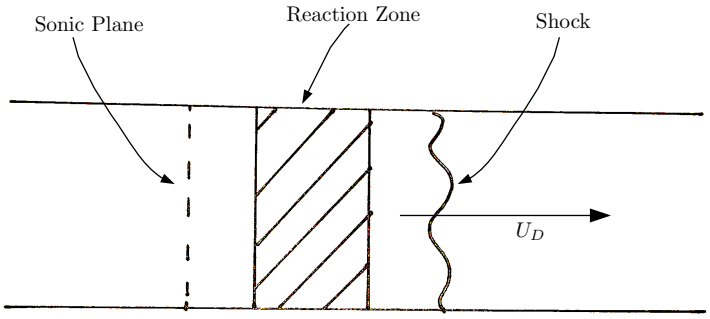

Figure 2: Basic 1D structure of a propagating detonation

exhibits a piecewise-smooth lead shock, transversely propagating shock waves and discontinuous reaction zones. The intersection points of the lead and transverse shocks generate high pressure and high vorticity regions that trace out a diamond-shaped pattern in the direction of propagation. The size of this diamond-shaped pattern is a property of a fuel mixture and its initial pressure: the detonation cell size λ. The cell size is a fundamental property of a detonation wave that dictates its propagation dynamics. When the space through which a detonation can propagate is restricted its velocity drops. Increasing the confinement of the detonation to the point where its velocity $U \approx 0.6 - 0.8U_{CJ}$ will typically cause the detonation to fail [5]. In micro-channels, this is due to the mass divergence in the boundary layer.

The pressure rise through the shock that occurs with detonations eliminates the need to pre-compress the reactants, leading some researchers to refer to this process as a method of pressure gain combustion (PGC). The large pressure gain through the shock also translates to a theoretically higher thermodynamic efficiency when compared to the RDEs constant pressure counterparts [2].

1.3 Early Work on Rotating Detonations

The original concept of what would become the RDE was proposed in 1959 by Voitsekhovskii in [6, 7] and summarized by Bykovskii in [8]. This first investigation of rotating detonations was done experimentally using a toroidal combustor into which a fuel mixture was injected radially. In parallel to this work, an American group led by Nicholls in the 1960s suggested that violent instabilities observed in engine concepts at the time could be harnessed for propulsion [9]. At the time, work on the structure of detonation waves had only recently begun and was absent from the initial concepts for the RDE. Though the knowledge of rotating detonations was limited, some of the RDE's key advantages were already known: the RDE has the potential to minimize the size of rocket combustors which can lead to significant gains in terms of launch weight, and it also has the proper configuration for a plug nozzle or aerospike type nozzle. Adamson Jr. [10] and Shen [11] continued the studies started by Nicholls by investigating the propagation of tangential waves in annular combustors.

1.4 RDEs and Detonation Properties

The detonation structure inside RDEs is similar to the structure of single-head spinning detonations in cylindrical tubes [12]. In these experiments, detonations have been observed propagating in spiral patterns along the walls of the tube, as opposed to RDE detonations which propagate in a circular pattern on the same plane inside of the flow field. After the early work on the RDE concept, the development of the engine stagnated until it was picked up by Bykovskii in the early 1980s [8]. This study hinted at the existence of a lower stability limit for rotating detonations and led to the development of the first detonation behaviour model for RDEs. This study was pushed further by Bykovskii in [13] when he observed the existence of roughly 3 detonation cells across the thickness of an RDE annulus. Bykovskii continued this work in 2006, when he established the first correlations between the detonation cell size λ and engine geometry [14]. These correlations are still widely used in RDE design today, and stipulate that the total length of fuel injected into an RDE combustor (L_{cr}) before it is consumed by the detonation front is $L_{cr} = (12 \pm 5)\,\lambda$, and the annulus thickness can be described as a function of the critical injection length L_{cr} where $h \approx 0.2 L_{cr}$. Furthermore, the minimum outer diameter of the combustion annulus is described as $D_o \approx 40\lambda$. These correlations can be seen as the starting point for modern RDE development.

1.5 Modern Development of RDEs

The work spearheaded by Bykovskii led to a large rise in interest in the development of RDEs as a combustion and propulsion concept. In the years since the RDE has been studied as a propulsion concept by Lu and Braun [3] as well as Kasahara [15], the latter of which is working in collaboration with the Japan Aerospace Exploration Agency (JAXA) in an effort to launch an RDE as the second stage of a sounding rocket in the early 2020s. Other notable work was done by Wolanski, who described the number of detonation waves travelling inside an RDE annulus as a function of the

engine's size[16]. Wolanski also studied the advantages of the RDE compared to other combustion concepts, including the pulse detonation engine and ramjet engine [1].

In recent years, much of the work in RDE development has focused on defining the occurrence of instability modes inside the RDE. These instabilities often take the form of two counter-rotating waves which appear to bounce off each other, in what is sometimes dubbed the clapping mode. Other instabilities as described by Annand are referred to as the chaotic instability, or the waxing and waning instabilities. [17]. These instabilities are characterized by a very irregular pressure pattern inside the RDE, which is indicative of the presence of detonations that fail and reignite themselves (galloping detonations) or possibly discrete ignition points inside the annulus with little to no propagation of a detonation wave. Experimentally, the occurrence of these instabilities can be mapped out for a given engine and fuel mixture giving other researchers a starting point for the development of their own engines. Another one of the main challenges in RDE design is engine cooling. The issue of engine cooling has meant that RDEs are currently unable to fire for more than a few seconds at a time. As there is currently no simple means of cooling RDEs, therefore the bulk of the heat generated inside the combustor is absorbed by the engine [18].

1.6 Current Work

Though the last two decades have seen research groups around the world work on the RDE, there is still a lack of understanding about how to design an RDE. Through experiments, researchers have been able to partially map out the stable operating conditions for a given RDE, as well as map out the occurrence of potential instability modes that may occur inside the engine. As of yet, there is no way to predict how an RDE of any given size, running on any given fuel mixture will operate. This thesis explores an analytical model that combines both the principles of compressible flow and basic detonation properties. Chapter 2 will describe how an RDE can be modelled geometrically and will detail the notions of compressible fluid mechanics present inside the engine. Chapter 3 will cover the notions of detonation physics important for RDE development. Chapter 4 will show how the notions described in chapters 2 and 3 can be combined into a coherent model to predict the stable operating map of an RDE and will compare the model's performance to real experimental data collected by Russo in 2011 and Hansmetzger in 2018 [19] [20].

Chapter 2

Geometric RDE Conditions and Flow Properties

At the present time the development of the RDE has mostly relied on the use of rules of thumb accepted in the community, and experiments that seem to have led RDE development to converge toward similar fuels and engine sizes. Though some researchers have used experiments to map out the mass flow rates for the stable operation of an RDE as well as certain instabilities, there exists no way to predict how a given engine will operate. The development of such a model would be critical in cutting the required time to design an RDE. A number of researchers have described certain geometric conditions such as the number of waves travelling inside an RDE annulus [16], however, to date no one has combined these geometric constraints with the principles of compressible flow and simple notions in detonation physics to create a coherent 1D model capable of predicting the operating modes of an RDE. The model developed over the course of this project combines both 1D isentropic flow as well as detonation physics with engine scaling. This chapter will focus on the model's geometric constraints, and how they affect the compressible flow field.

2.1 Modelling of Geometric Conditions

The RDE combustor operates as a thin annulus inside of which any number of detonation waves can exist. First, we define the number of detonation waves ω inside the annulus as the ratio of the combustor's circumference to the number of waves inside the annulus. In fig. 4a, we see two different length scales: $L_{cr} \approx (12 \pm 5)\lambda$ and $h > 2.5\lambda$. The former of these was determined in [14], and the latter is a rule of thumb based on the former. In [14], Bykovskii describes the annulus thickness h as a function of the critical injection length L_{cr} such that $h \approx 0.2L_{cr}$. From this we introduce a proportionality constant $C = 5$.

$$L_{cr} \geq Ch \tag{1}$$

This proportionality constant implies the following relationship for the aspect ratio h/λ.

$$\frac{h}{\lambda} = \frac{12 \pm 5}{5} = 2.4 \pm 1 \tag{2}$$

The lower limit of this relationship approaches the minimum operability limits of the RDE, and therefore the accepted rule of thumb in RDE design has been that the aspect ratio must be

$$\frac{h}{\lambda} \geq 2.5. \tag{3}$$

From here, it is useful to describe the spacing between two consecutive detonation fronts in 2D by "unwrapping" the annulus as seen in fig. 4b. Here we show the spacing between two moving detonation fronts separated by a growing area of fresh reactants. The reactants form a triangle between the two detonations, where the spacing between the two waves is $\pi D/\omega$, and the final length of fuel mixture injected into the annulus is $L_{cr} = (12 \pm 5)\,\lambda$. These lengths can be equated to the ratio of reactant injection velocity V_{inj} to detonation velocity U_D to determine the number of waves travelling inside the annulus by taking the tangent of the angle θ shown in fig. 4b.

$$\tan\theta = \frac{V_{inj}}{U_D} = \frac{L_{cr}}{\frac{\pi D}{\omega}} \tag{4}$$

Equation 4 can be further developed by including the definition of the mass flow rate $\dot{m} = \rho V_{inj} A$ where the area $A = \pi D h$. By cancelling out the appropriate terms, this yields the following expression for the wave number ω.

$$\omega = \frac{\dot{m}/\rho}{h U_D L_{cr}} \tag{5}$$

This equation can be further simplified by assuming the reactants are ideal gases with $PV = \rho RT$ to eliminate the density ρ. The extent of the detonable zone is also assumed to scale with the detonation cell size as $L_{cr} = C_L \lambda$.

$$\omega = \frac{\dot{m} R_s T}{C_L \lambda P U_D h}, \tag{6}$$

We now include how the detonation cell size scales with the pressure of the detonable mixture. The cell size normally scales with pressure following an inverse relationship

$$\frac{\lambda}{\lambda_{ref}} = \left(\frac{P_{ref}}{P}\right)^m \tag{7}$$

where typically $m = 1$. This equation then implies

$$\lambda P = \lambda_{ref} P_{ref} \tag{8}$$

where λ_{ref} is the detonation cell size at a given reference pressure, typically $P_{ref} = 100$kPa .The estimation of the cell size is developed in greater detail in section 3.1. We include the result of this estimation in equation 6 to give a final expression for the wave number.

$$\omega = \frac{\dot{m} R_s T}{C_L \lambda_{ref} P_{ref} U_D h}, \tag{9}$$

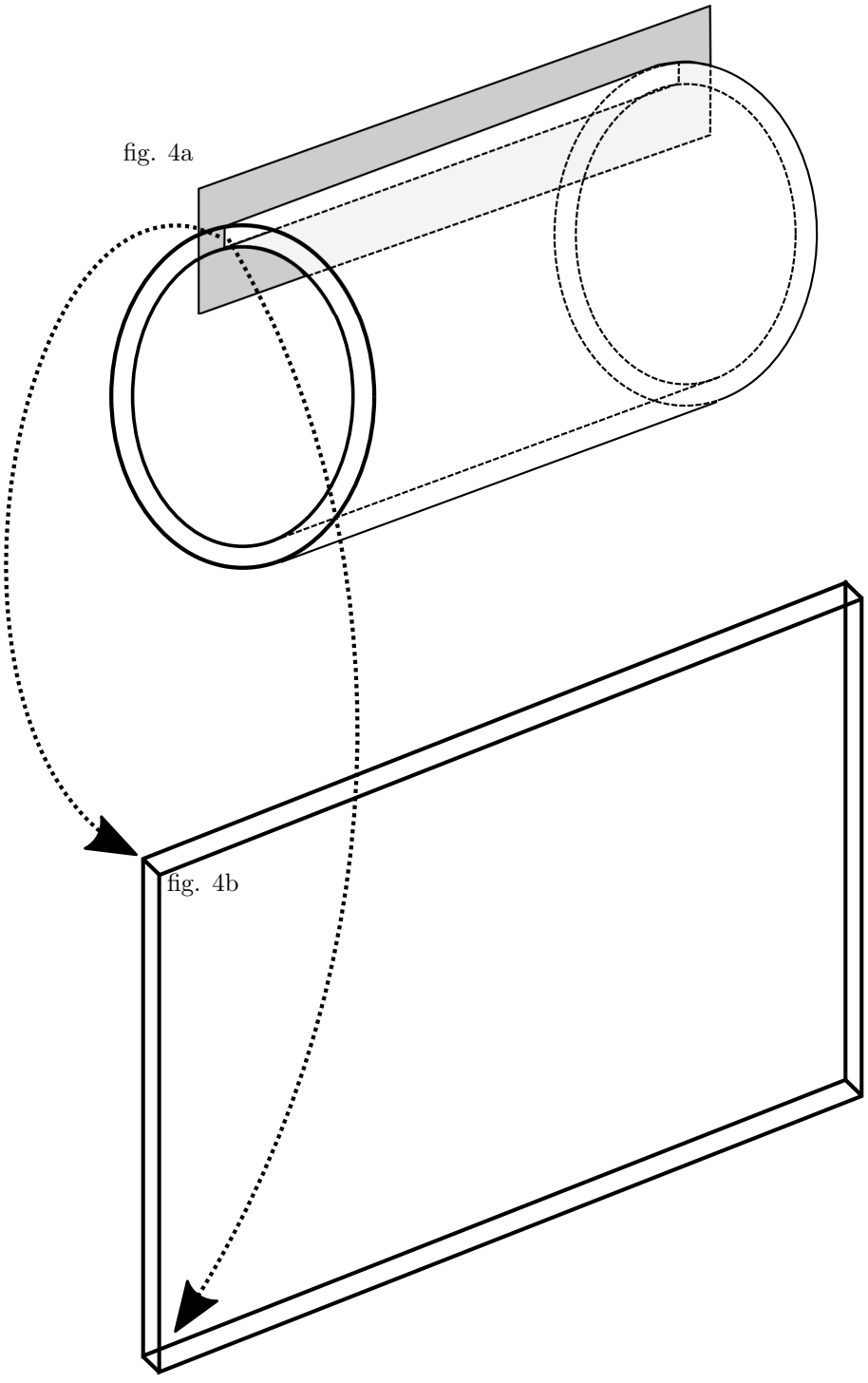

Figure 3: View of the RDE annulus and cutting plane, normal to the view in fig. 4a. Unrolled annulus showing the 2D representation on which fig. 4b is based.

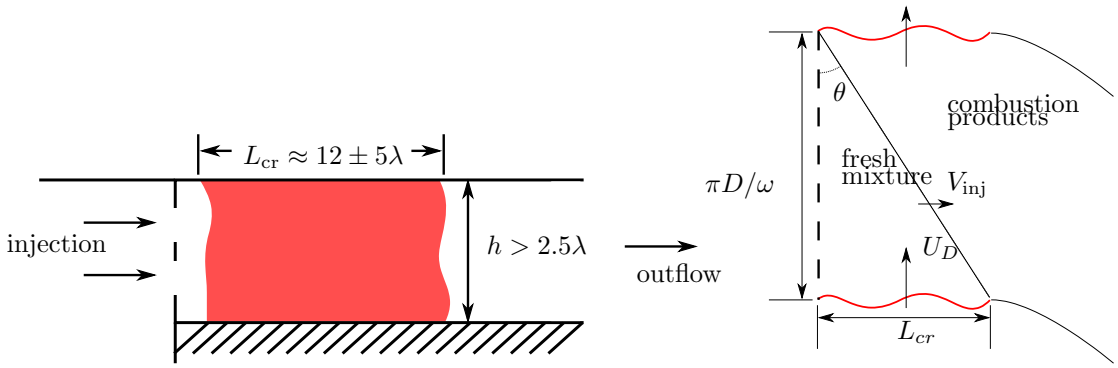

(a) RDE cross-sectional view of combustor, showing detonation front in red

(b) Unwrapped RDE annulus

Figure 4: 4a: Annular combustion chamber cross-section showing the detonation (traveling into the page) region in red. The injection ports are on the left and combustion product outflow is on the right. The hatched body below the detonation is the RDE's centre body. 4b: Unwrapped combustion chamber section showing two detonations (in red) following each other with injection ports on the left side. Both detonations are a top view of the detonation shown in fig. 4a.

2.2 Modelling of Flow Field Using Compressible Fluid Dynamics

To close the model, the flow field properties inside the RDE annulus need to be estimated. When investigating what the flow properties would be inside the annulus before the shock, the RDE's injector was assumed to be choked and represented by a converging-diverging isentropic nozzle. This left a few possibilities with regard to the flow field. The fuel mixture could either: expand supersonically, expand back to the subsonic regime, or expand supersonically and encounter a normal shock. These three possibilities have been investigated, and the final pre-detonation pressures inside the chamber were compared to [21]. This engine is 150 mm in outer diameter with a 5 mm annulus thickness h. The fuel mixture used was a methane-oxygen mixture flowing at a mass flow rate of $\dot{m} = 0.210$ kg/s, an equivalence ratio $\phi = 1.65$ and with a total pressure of 7 bar (700 kPa). First, the mixture's gas properties $R_{s,mix}$ and γ_{mix} are found using the reactants mass fractions Y_i found from balancing the following stoichiometric equation

$$\phi \mathrm{CH_4} + 2\mathrm{O_2} \rightarrow (2-\phi)\mathrm{CO_2} + 2\phi \mathrm{H_2O} + (2\phi - 2)\mathrm{C}, \phi \geq 1, \tag{10}$$

where $\phi = 1.65$. Next, the mass fractions of each reactant Y_i are computed, and the mixture's specific gas constant $R_{s,mix}$ and ratio of specific heats γ_{mix} are computed using a method of mass weighted averages. The results of these calculations are shown in table 1.

The specific gas constant of the mixture could also have been computed using the molar mass of the mixture, however to simplify calculations the mass-weighted average method was used for both $R_{s,mix}$ and γ_{mix}. With these flow properties, we can begin using the isentropic flow equations for a flow field involving this fuel mixture. Next, we find the area A^* required to choke the flow at 0.210 kg/s and 700 kPa, and assuming a stagnation temperature $T_0 = 293$K using the definition for the

Table 1: Gas properties for reactant species and fuel mixture

	CH_4	O_2	Mix $\phi = 1.65$
Y_i	0.295	0.705	
$R_{s,i}\left(\frac{J}{KgK}\right)$	518.28	259.84	336.08
γ_i	1.32	1.4	1.376

Table 2: Chamber pressure solutions and their percent difference from the Kindracki experiment

	P_{cc}(kPa)	%Δ
Subsonic solution	698.22	619.8
Supersonic solution	5.82	94.0
Normal shock solution	96.05	0.98
Kindracki experiment	97	

mass flow rate through a choked orifice.

$$\dot{m} = A^* P_0 \sqrt{\frac{\gamma}{R_{s,mix} T_0} \left(\frac{\gamma+1}{2}\right)^{\frac{\gamma+1}{1-\gamma}}} \tag{11}$$

Knowing the cross-sectional area of the RDE's annulus, we can use a simple root finding method to calculate the Mach number M_{inj} of the fuel mixture injected into the annulus using the compressible area ratio equation.

$$\frac{A}{A^*} = \left(\frac{2}{\gamma+1}\right)^{\frac{\gamma+1}{\gamma-1}} \frac{1}{M_{inj}} \sqrt{\left(1 + \frac{\gamma-1}{2} M_{inj}^2\right)^{\frac{\gamma+1}{\gamma-1}}} \tag{12}$$

This equation has two valid solutions: $M_{inj} < 1$ and $M_{inj} > 1$. In this case, we will be investigating the properties at both conditions. Once M_{inj} is found, we can then calculate the static pressure P_{inj} of the fuel mixture as it is injected into the annulus using the isentropic pressure ratio equation.

$$\frac{P_{inj}}{P_0} = \left(1 + \frac{\gamma-1}{2} M^2\right)^{\frac{\gamma}{1-\gamma}} \tag{13}$$

If the flow expands to the subsonic regime, P_{inj} is the pre-detonation pressure and will be denoted as P_{cc}. Likewise, if the flow expands to the supersonic regime and remains that way before encountering the detonation, we also have $P_{inj} = P_{cc}$. For the third studied case, the flow expands supersonically before encountering a normal shock wave at the exit of the injector. In this case, P_{inj} becomes the pre-shock pressure, and the desired annulus pressure P_{cc} is the post-shock pressure. P_{cc} is then calculated using the pressure ratio equation through a normal shock wave.

$$\frac{P_{cc}}{P_{inj}} = 1 + \frac{2\gamma}{\gamma+1}\left(M_1^2 - 1\right) \tag{14}$$

The results of this study compared to [21] are shown in table 2. Considering that the normal shock solution differs from Kindracki's experimental chamber pressures to within 1%, it became clear that the flow encountered a normal shock at the exit of the nozzle. As such, the flow field is represented by a converging-diverging isentropic nozzle with an outlet normal shock, as shown in fig. 5. A fuel mixture enters the RDE at a given stagnation pressure P_0 and at a given mass flow rate $\dot{m}$.

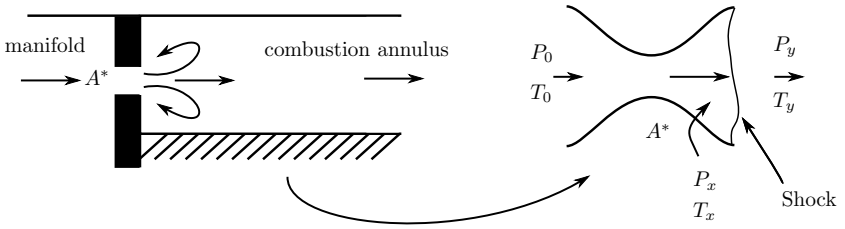

Figure 5: Schematic of a premixed RDE showing the simplification of the injection plane to a choked isentropic nozzle with equal throat area followed by a normal shock.

When injected into the annulus, the mixture chokes at the engine's injector before undergoing a supersonic expansion into the engine's annulus. To obtain the Mach number M of the fuel mixture injected into the annulus, we can use a standard root finding method on the compressible area ratio equation shown in equation 12. Once the Mach number of the flow exiting the injector is calculated, the pressure of the reactants at the exit of the injector, modelled here as a converging-diverging isentropic nozzle is found using the isentropic pressure ratio in equation 13.

Since the presence of detonations inside the annulus causes a pressure rise, they can be seen as an elevated back pressure. According to the principles of compressible flow, higher back pressure will cause the introduction of a normal shock wave at the exit of the RDE injector. The normal shock forces the flow field back to subsonic and increases the static pressure according to equation 14, where P_{ch} denotes the pressure of the fuel mixture inside the annulus ahead of the detonation.

Once the flow properties ahead of the detonation are known, it is possible to estimate the detonation properties of a given fuel mixture.

Chapter 3

Estimating Detonation Properties at Extreme Conditions

The model developed thus far consists of two parts. The first is a dynamic balance between (1) the injection and detonation speeds and (2) the extent of the detonating zone and the detonation travel path. This balance leads to the determination of the wavenumber as described in chapter 2. The second part is the scaling of the annular combustion chamber thickness with the detonation cell size. Underpinning these two relationships are the characteristic detonation speed U_{CJ} and the detonation cell size λ. Evaluating these parameters as a function of the initial reactant temperature, pressure and composition is essential to properly model the behaviour of rotating detonation engines.

3.1 Estimation of Detonation Cell Size

There is currently no clear-cut way to calculate the expected size of detonation cells through analytical means. Therefore, the most direct way to estimate the detonation cell size λ of a given fuel mixture is to run a series of soot foil experiments to measure cell sizes for given fuel mixtures at the expected pre-detonation pressures calculated in section 2.2. These experiments, however, are time-consuming and require an apparatus capable of handling a detonation experiment with initial static pressures of 100 to 200 kPa as is expected inside of an RDE. Instead, this model relies on experimental data from the GALCIT Detonation Database [22]. GALCIT is able to provide researchers with experimental data on a variety of fuels ranging in size from hydrogen (H_2) to hexane (C_6H_{14}), and with oxidizers such as pure oxygen (O_2), air ($O_2 + 3.76N_2$) as well as diluted oxygen-based mixtures ($O_2 + xN_2$/Ar...). These results are accessible as plots and data tables of detonation cell size vs. the fuel equivalence ratio ϕ, the mixture's initial pressure, or the proportion of diluent used. For this study, however, some of the studied fuel mixtures do not have any specific data available in the detonation database. It was therefore necessary to use estimations for the detonation cell sizes using a series of curve fits and extrapolations described in the following method. The example detailed below will involve H_2 and an oxygen-enriched air mixture.

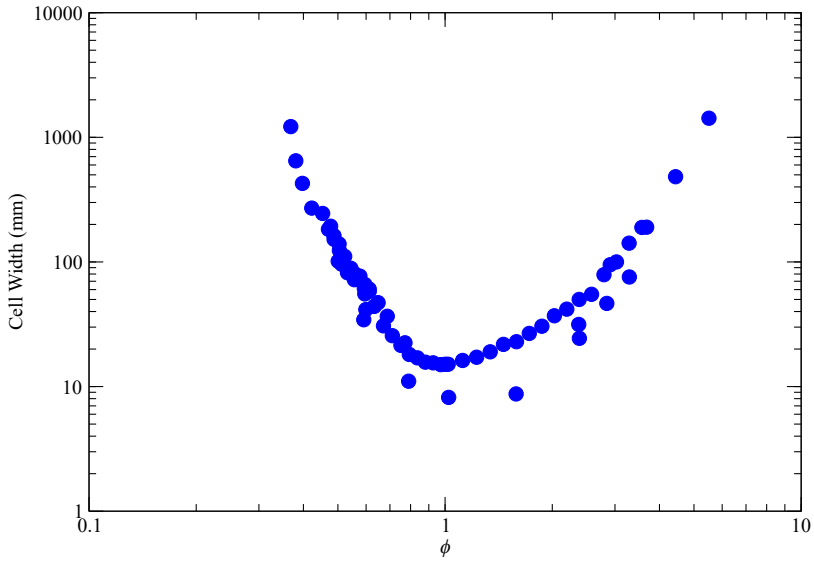

Figure 6: Experimental cell sizes of a H_2+ Air fuel mixture

First, similar fuel mixtures are found in the detonation database. In this case, oxygen enriched air falls between a pure air mixture and a pure oxygen mixture. Data sets detailing λ vs. ϕ exist for H_2-air at 101.325 kPa initial pressure, as shown in fig. 6. For H_2 + O2, only the cell size at stoichiometric conditions is known. The variation of cell size against equivalence ratio is not known at all dilutions. If there is no other way to estimate a cell size for the desired fuel mixture, it is possible to perform a linear interpolation to give an estimation of what the expected cell size should be at any equivalence ratio, for any dilution. In this case, there exists data for λ vs. the percentage of N_2 diluent in the mixture. Using a curve fit on this data set as shown in fig. 7, it is possible to estimate λ at 101.325 kPa for the desired fuel mixture. In this case, the curve fit is shown in equation 15.

$$\lambda = 1.105e^{0.0404\%\mathrm{N_2}} \tag{15}$$

This value is denoted as λ_{ref} at a pressure $P_{ref} = 101.325$ kPa for the stoichiometric mixture. Using the nitrogen dilution ratio from [19] in equation 15, we find that $\lambda_{ref} = 9.35$ mm. Once this value is obtained, we return to the data sets showing λ vs. ϕ for a mixture of hydrogen and air in fig. 6. In this case, we restrict ourselves to a range of equivalence ratios corresponding to the experiments in [19], namely $0.85 \leq \phi \leq 1.34$. The resulting curve fit for this range of equivalence ratios is shown in fig. 8 and equation 16.

$$\lambda = 38.47\phi^2 - 78.21\phi + 55.02 \tag{16}$$

Next, we find the ratio between the stoichiometric cell size of H_2+air and the previously calculated λ_{ref}, i.e. the stoichiometric cell size of the target mixture. We then implement this ratio on the

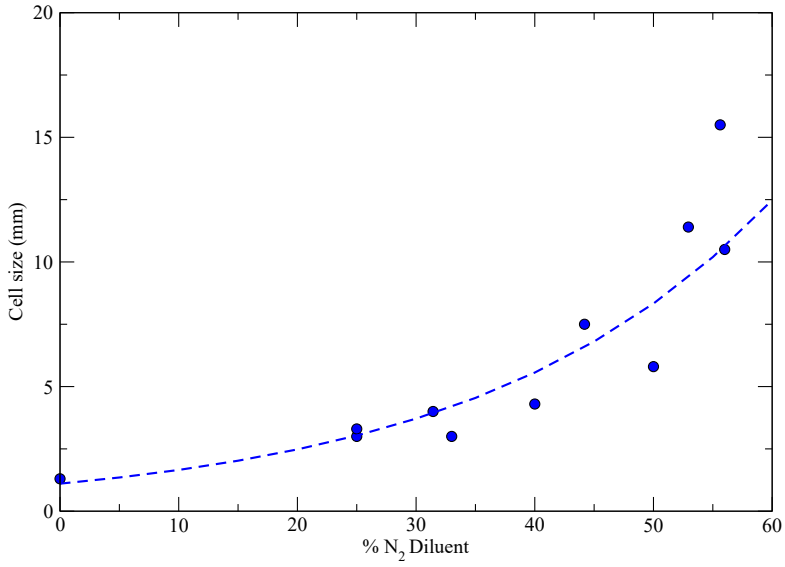

Figure 7: Experimental cell sizes of a $H_2 + O_2 + N_2$ vs. % Dilution of N_2 with curve fit (dashed line)

entire $\lambda(\phi)$ curve fit shown in fig. 8, which leads to the cell size extrapolation shown in fig. 9.

This method yields an estimation of the fuel mixture's behaviour at P_{ref} for a range of equivalence ratios, for which exact values are shown in table 3. Finally, the effect of the mixture's initial pressure must be taken into account. Using the λ vs initial pressure plots, we can estimate how the mixture will react to different initial pressures. These data sets are shown on logarithmic plots and, generally, the behaviour is very close to being inversely proportional to pressure, as shown in fig. 10, such that

$$\lambda = \lambda_{\text{ref}} \frac{P_{\text{ref}}}{P}. \tag{17}$$

Combining both $\lambda(\phi)$ and $\lambda(P)$ allows the estimation of a fuel mixture's cell size with respect to varying equivalence ratios and initial pressures.

3.2 Estimation of Detonation Velocity

The expected detonation velocity is the final property needed to predict the operation mode for a given RDE running on a known fuel mixture. Here, the theoretical detonation velocity U_{CJ} can be calculated using a chemical equilibrium code such as CEA provided by NASA. This velocity corresponds to the maximum expected velocity that an unimpeded and unsupported detonation can attain. RDEs, however, have three major characteristics that can slow down the detonation velocity U_D below U_{CJ}. First, the detonations travelling inside the annulus are forced to follow a curved path, which results in a slight curvature and a correspondingly small decrease in detonation speed. Second,

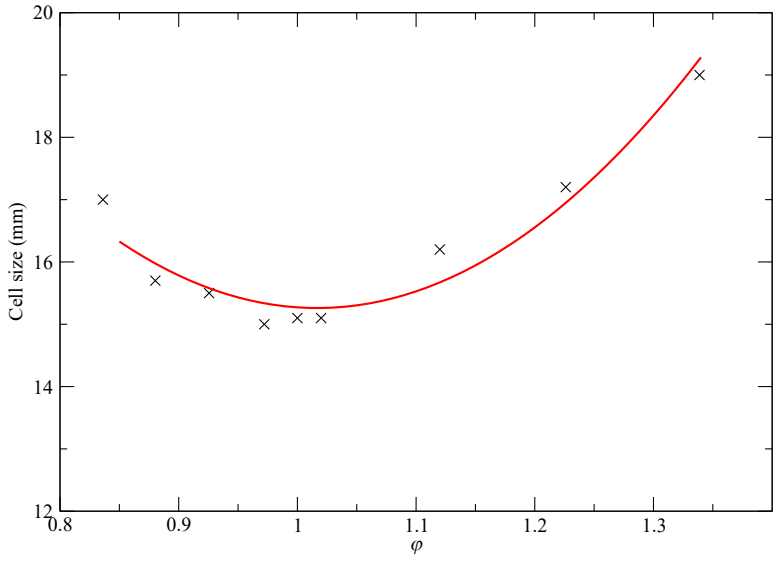

Figure 8: Curve fit on H_2+ air λ vs ϕ data

the thin annular nature of the RDE combustor acts as a thin confinement. The boundary layers on the confinement walls are large with respect to the confinement length scale. These boundary layers result in wave curvature across the annulus thickness and a corresponding decrease in detonation velocity. Third, the gases are expanding towards the outlet of the engine, which leads to a curved detonation front along the engine axis, a lowered pressure, and a velocity decrement. The behaviour of a detonation inside an RDE can be seen as analogous to the behaviour of detonations in curved microchannels. As such, these kinds of experiments were considered when estimating the detonation velocities inside RDEs. Fig. 11 shows an example of how increasing the curvature experienced by a detonation can slow its propagation speed [23]. For so-called regular detonation waves (typically mixtures with high Ar dilutions), the velocity decrement follows that predicted by the nozzled detonation solution shown in fig. 11a. Detonation failure occurs when $U_D \approx 0.8 - 0.9U_{CJ}$. For irregular mixtures (fuel-air, fuel-O_2 and N_2 diluted mixtures among others) the wave can sustain a higher velocity loss (see fig. 11b. Failure typically occurs around $U_D \approx 0.65 - 0.7U_{CJ}$.

Studies on the behaviour of detonations in microchannels have pointed to certain areas of detonation stability defined by the overall measured detonation velocity[5]. This paper describes a series of experiments studying detonations in micro-channels with the specific goal of simulating RDE conditions. Three different regimes have been identified: stable detonations that travel at over 80% U_{CJ}, critically stable detonations that travel between 60 and 80% U_{CJ}, and unstable detonations which travel under 60% U_{CJ}. Detonation phenomena are still possible in the unstable regime, however, it is more likely that the reduced speed in this regime is caused by the presence of an instability such as galloping detonations, or in the case of the RDE we see two counter-rotating waves travelling

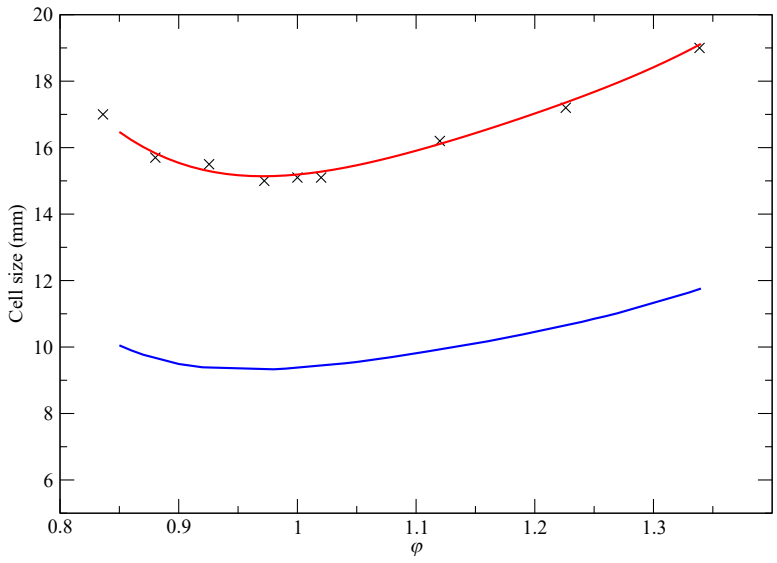

Figure 9: Curve fit on H_2+ air λ vs ϕ data (red) and extrapolation for enriched air mixture (blue)

inside the chamber. The detonation velocity is expected to be a function of the wave's confinement in all directions, of a form similar to:

$$\frac{U}{U_{CJ}} = f\left(\frac{h}{\lambda}, \frac{L_{cr}}{\lambda}\right) \tag{18}$$

In the present RDE model, we attempt only to calculate the lowest possible mass flow rate corresponding to the limit condition of the detonation wave's stability. In other words, we are evaluating the operation of the engine when the continuously rotating detonation is near its failure limit. In this case, we impose a constant velocity decrement of

$$\frac{U}{U_{CJ}} = 0.6, \tag{19}$$

to match with the minimum "critically stable" detonation velocity as defined by Kudo in [5]. Note that Kudo's work used $C_2H_4 + O_2$, an irregular mixture consistent with a high velocity decrement. Evaluating relation 18 would make this model applicable to all conditions of $\dot{m}$ and ω.

Table 3: Reference cell size vs. equivalence ratio for the studied fuel mixture

ϕ	λ_{ref}
0.85	10.05
0.86	9.9
0.87	9.77
0.9	9.49
0.92	9.39
0.98	9.33
0.99	9.35
1.04	9.51
1.05	9.55
1.08	9.7
1.11	9.87
1.12	9.93
1.13	9.99
1.15	10.11
1.16	10.17
1.17	10.24
1.19	10.38
1.24	10.76
1.25	10.85
1.26	10.93
1.27	11.02
1.33	11.64
1.34	11.76

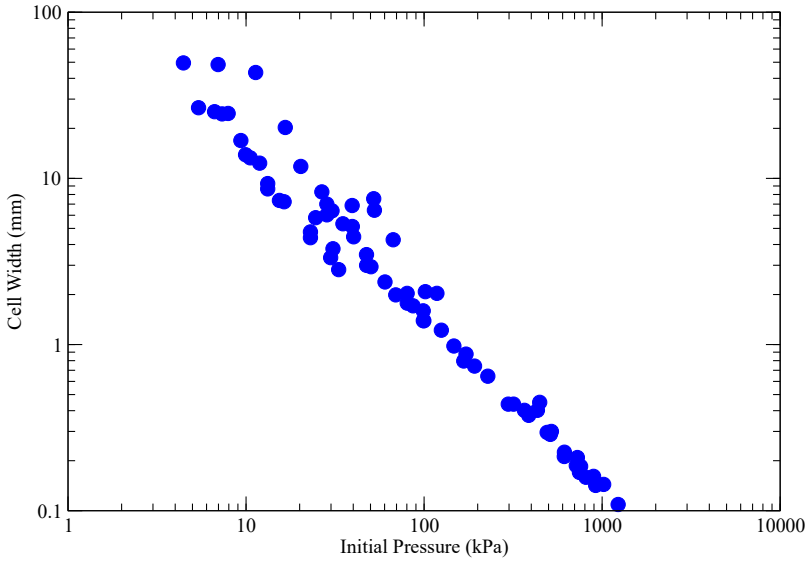

Figure 10: Experimental cell sizes of a $H_2 + O_2$ vs. initial mixture pressure

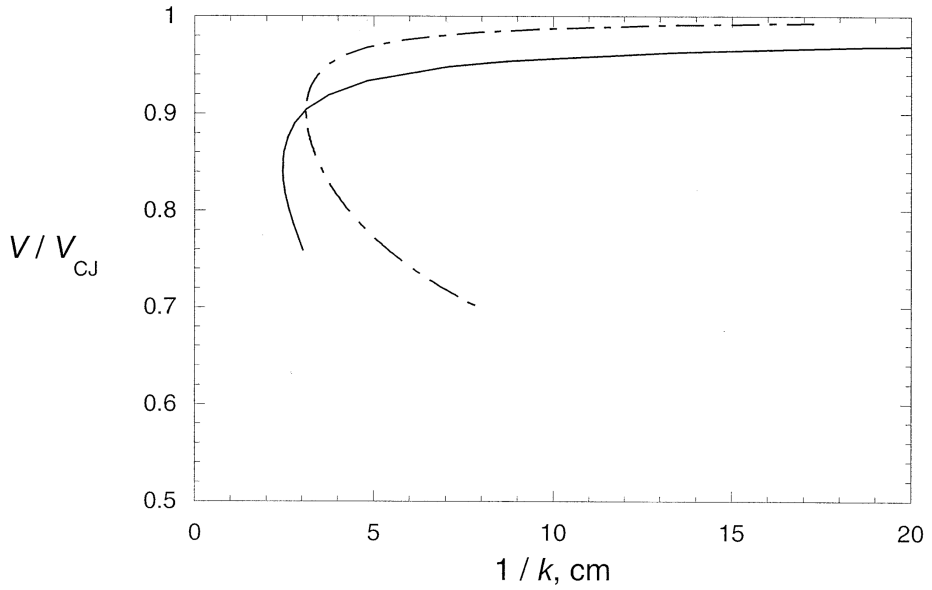

(a) Detonation wave velocity dependence on frontal curvature κ for $C_2H_2 + 2.5O_2 + 75\%Ar$ [23]

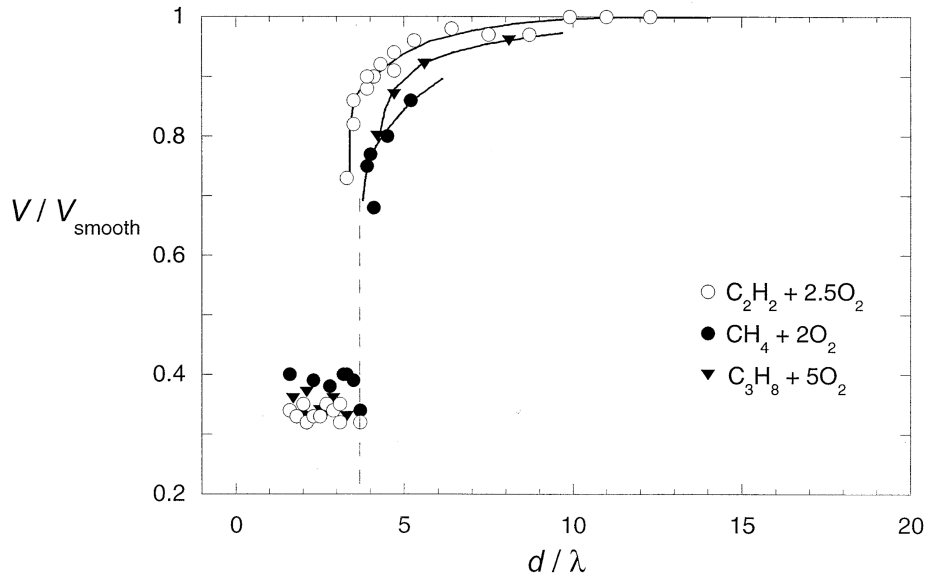

(b) Detonation wave velocity dependence on diameter, in contact with a porous medium

Figure 11: Examples of typical velocity decrements due to the effects of curvature in fig. 11a and porous surroundings in fig. 11b

Chapter 4

RDE Prediction Model Results and Validation

This chapter will focus first on how combining the principles of compressible flow and detonation physics can help researchers design an RDE of any given size. Once this process has been detailed, this method will be applied to two existing RDEs in an attempt to reproduce results obtained by two separate research teams: the United States Air Force RDE running on hydrogen and oxygen-enriched air developed by Russo, and the RDE at Institut PPrime in Poitiers, France running on ethylene, oxygen and nitrogen diluted mixtures.

4.1 Designing an RDE by Combining Compressible Flow & Detonation Physics

As discussed previously, the RDE model operates by combining the principles of compressible flow and detonation physics detailed in chapters 2 and 3 into a simple, analytical model. At any given mass flow rate and engine size, an RDE will exhibit an intrinsic wave number ω and a given relative annulus thickness h/λ. These two parameters are subjected to the geometric constraints described in section 2.1.

$$\omega \geq 1 \tag{20}$$

$$h/\lambda \approx 2.4 \pm 1 \tag{21}$$

In short, an RDE must be able to sustain at least one detonation wave travelling inside the annulus, and to operate in a stable mode the annulus must be thick enough to support roughly 2.4 detonation cells across its width. As an absolute minimum for stable operation of an RDE, the relative annulus thickness is as follows

$$h/\lambda \geq 1, \tag{22}$$

i.e. the RDE's annulus must be able to support at least one detonation cell across its annulus thickness. The limits described in equations 20 and 22 form the basis for predicting the minimum

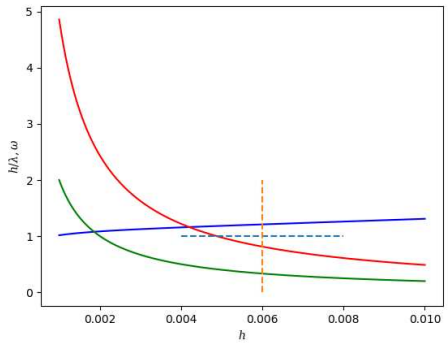

(a) A non-valid solution for a 6mm annulus RDE.

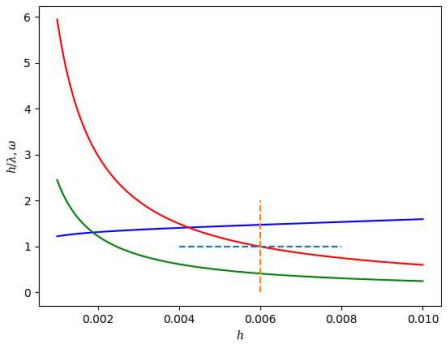

(b) A 6mm annulus RDE at its minimum mass flow conditions

Figure 12: Prediction model results showing minimum expected (green) and maximum expected (red) wavenumber, along with the expected number of cells across h (blue) for a range of annulus thicknesses. An RDE with $h = 6$mm (orange dashed line) and $h/\lambda = 1$ & $\omega = 1$ (blue dashed line) is identified.

mass flow rate to operate an RDE of any given size. To help with the design of an engine of a given diameter running at a specific fuel mixture, this model allows a user to predict the expected number of detonation waves inside the engine and the number of detonation cells across the RDE's annulus for a desired mass flow rate.

Sample results are shown in fig. 12 for an engine with a 70 mm outer diameter D_o, an annulus thickness $h = 6$ mm running on hydrogen and oxygen-enriched air with a stagnation pressure $P_0 = 5516$ kPa (800 psi). The engine geometry and flow conditions used in this example match the experiments run by Russo in 2011 [19], and will be used to validate the performance of this model in section 4.2. In fig. 12a, the minimum conditions are shown by a horizontal dashed line, and the desired annulus thickness is shown by the vertical dashed line at 6 mm. The green and red curves represent the lower and upper expected limit for the wavenumber, and the blue curve describes the expected aspect ratio h/λ vs. h. This figure shows that while the engine operates at a mass flow rate that would be able to accommodate one detonation cell across the annulus, the flow rate is too low to be able to sustain at least one detonation wave around the circumference of the engine. Using a simple root-finding method, we can iterate on the mass flow rate until it reaches the critical limit shown in fig 12b, where the engine can accommodate one detonation cell across the annulus and can sustain a maximum of one detonation wave inside the annulus. In short, the mass flow rate obtained after iteration is the minimum mass flow rate for this given engine running on a specific fuel mixture and equivalence ratio. To know the overall behaviour of a given engine, we extend this study to multiple equivalence ratios as shown in fig. 13. Here, the blue curve shows the minimum expected mass flow rate for the stable 1 wave operation of the sample RDE for a range of fuel equivalence ratios ϕ. The flow rates are identified on the left in pounds per minute, and on the right in kilograms per second.

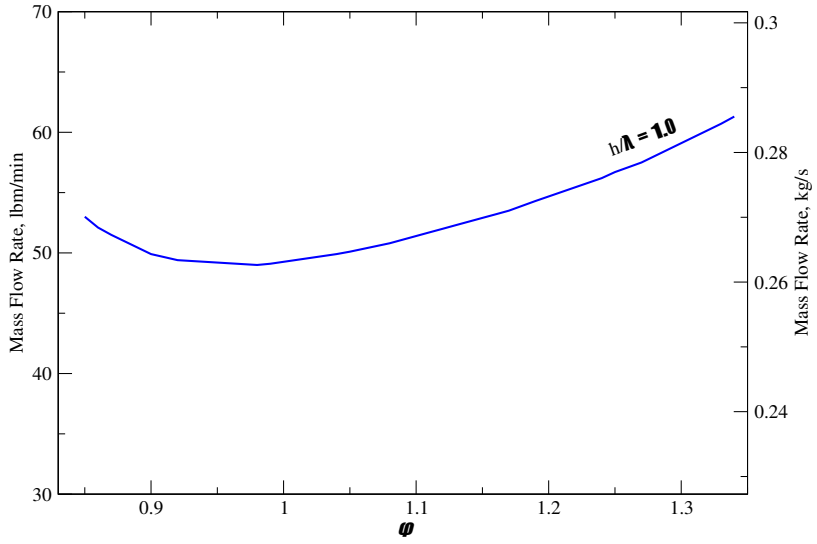

Figure 13: Minimum mass flow rate for a H2+ enriched air engine.

4.2 Air Force Institute of Technology RDE Running on H_2 + Enriched Air

In 2011, Russo and the Air Force Institute of Technology developed a 3-inch diameter engine with a 6 mm annulus running on hydrogen and oxygen-enriched air. These experiments were run near the operable limits of the RDE in question. The conclusions of this study were that a 3-inch RDE running on this fuel mixture should be run at a flow rate above 35 lbs/min to ensure the stable operation of the engine. To confirm the validity of the model, a set of cases were run showing the model's predictions for the minimum flow rate necessary to sustain one detonation wave for a range of relative annulus thicknesses h/λ, ranging from $h/\lambda \geq 2.5$ down to $h/\lambda \geq 1$. The results are shown in fig. 14. Represented by square symbols is the lowest mass flow rate, for a given equivalence ratio, at which a sustained RDE operation was observed by Russo [19], imposing simultaneously that $\omega = 1$ and $h/\lambda = K$ where $K = 2.5, 2.0, 1.5, 1.0$.

The test data collected by Russo corresponds closely to what is predicted by the model for $h/\lambda = 1$. This validates the use of $h/\lambda = 1$ as a limiting factor for RDE operation. Next, in fig. 15 we look more closely at how the data itself compares to the model's predictions.

We see that the model is able to predict the minimum operable flow rates for Russo's engine to a strikingly high degree of accuracy up until an equivalence ratio $\phi = 1.05$. At higher equivalence ratios, the data points become more erratic. This is likely caused by the large spread in measured detonation velocities during this experiment. In the cases at higher equivalence ratios where the data points differ largely from the model's predictions, the detonation velocities measured were under $0.55D_{CJ}$. This indicates that these tests were deemed successful but that the engine may have been operating under an instability mode such as galloping detonations or the often observed mode with 2 counter-rotating detonations sometimes called the "clapping" instability mode. As of yet, it is unclear whether the clapping instability is actually a desirable operating mode for RDEs. Whether

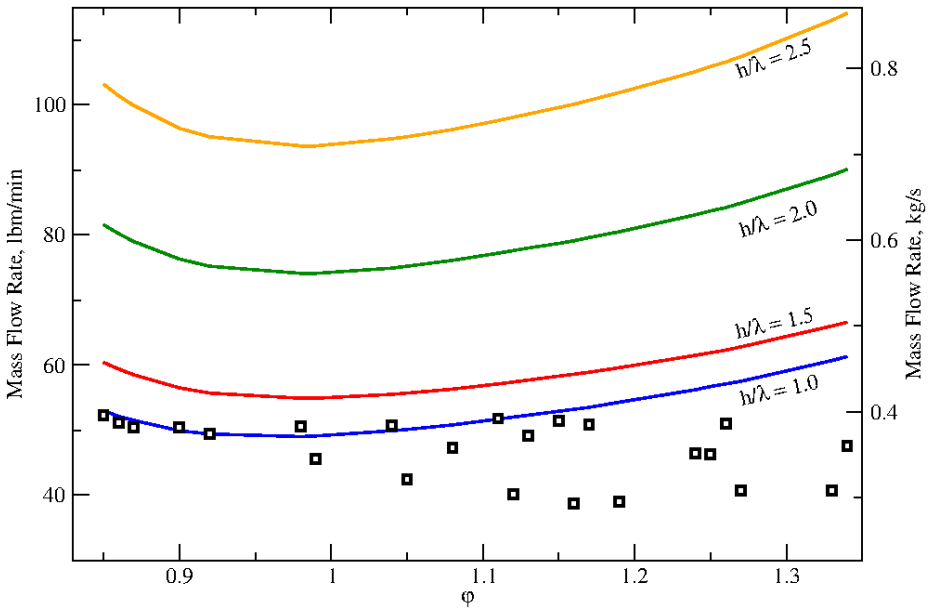

Figure 14: Varying values of h/λ compared to data collected by Russo (2011)

the physical interpretation of this mode is that two waves are observed either bouncing off of each other or passing through each other, the two waves should have no fuel to consume after interacting with each other. As such, this instability mode cannot be predicted by the model described in this document since its purpose is to predict the stable operating modes of the RDE. Even so, this model gives a good approximation of the lower operating bounds of Russo's RDE.

4.3 Institut PPrime RDE Running on $C_2H_4 + O_2 + N_2$ Based Mixtures

The model's performance was also tested against the RDE developed by Hansmetzger at Institut PPrime in Poitiers, France. This series of RDE experiments used $C_2H_4 + O_2$ based mixtures with a varying amount of N2 as a diluent for a range of fuel equivalence ratios. Also varied was the annulus thickness h with $h = 5$ mm and $h = 10$ mm. Hansmetzger also investigated the impact of a cylindrical and a conical centre body in the RDE however only the cylindrical combustor experiments will be considered to test the performance of the model. We begin by using the prediction model to find the minimum mass flow rates for ethylene and pure oxygen at various equivalence ratios for an engine with an annulus thickness of 10 mm. The comparison between the predictions and Hansmetzger's data for this engine are shown in fig. 16. Here the dotted line represents the minimum flow rates predicted by the model, the grey data points represent the clapping instability and the black data points represent successful $\omega = 1$, continuously rotating detonation tests. In this case, the prediction model shows good agreement with the test data near stoichiometric, however, the gap between the model and experimental data grows as we get farther from stoichiometric conditions. This is possibly due to the scarcity of detonation cell size data at different equivalence ratios for

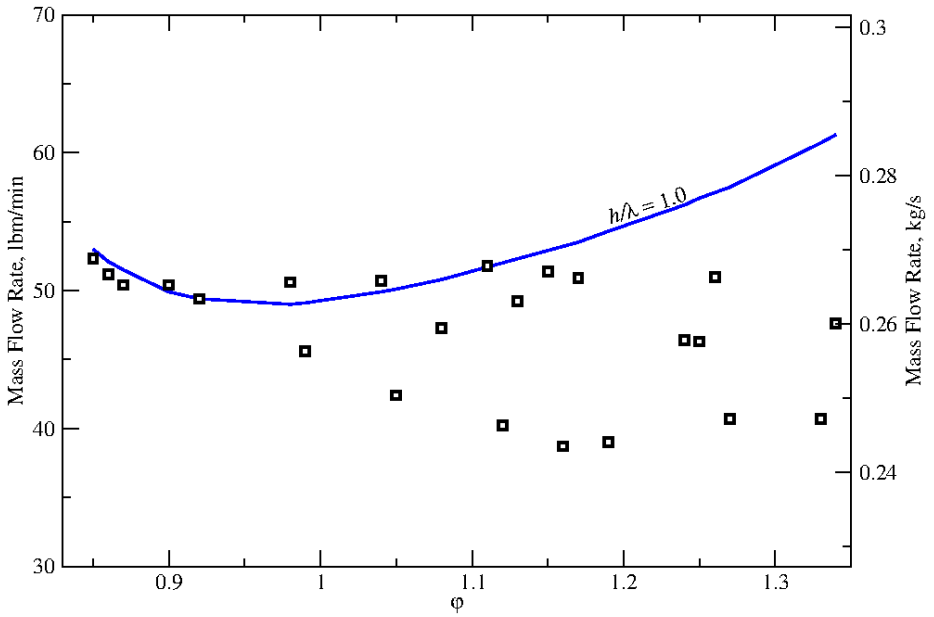

Figure 15: Limiting case with $h/\lambda = 1$ compared to data collected by Russo (2011)

C2H4 + O2 mixtures. With very little data available for these mixtures, the method described in chapter 3 is likely to introduce discrepancies in the model's predictions. Still, it is worth noting that all but one of the tests which yielded the clapping mode occur below the model's predictions. This would indicate that despite its deficiencies, the model is still able to approach the lower stability limit. Predictions for the different cases tested by Hansmetzger are shown in fig. 17.

Unfortunately, the data collected is insufficient to draw any conclusions with regards to the prediction model for the other cases tested by Hansmetzger.

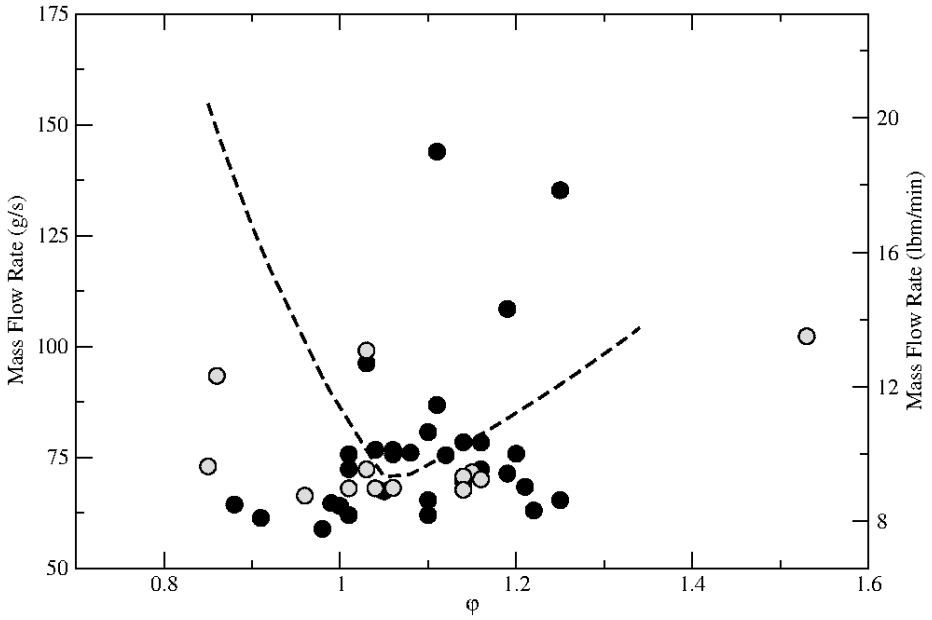

Figure 16: Comparing Poitiers data for $\beta = 0$ and $h = 10mm$ to the minimum mass flow rate model with $h/\lambda = 1$

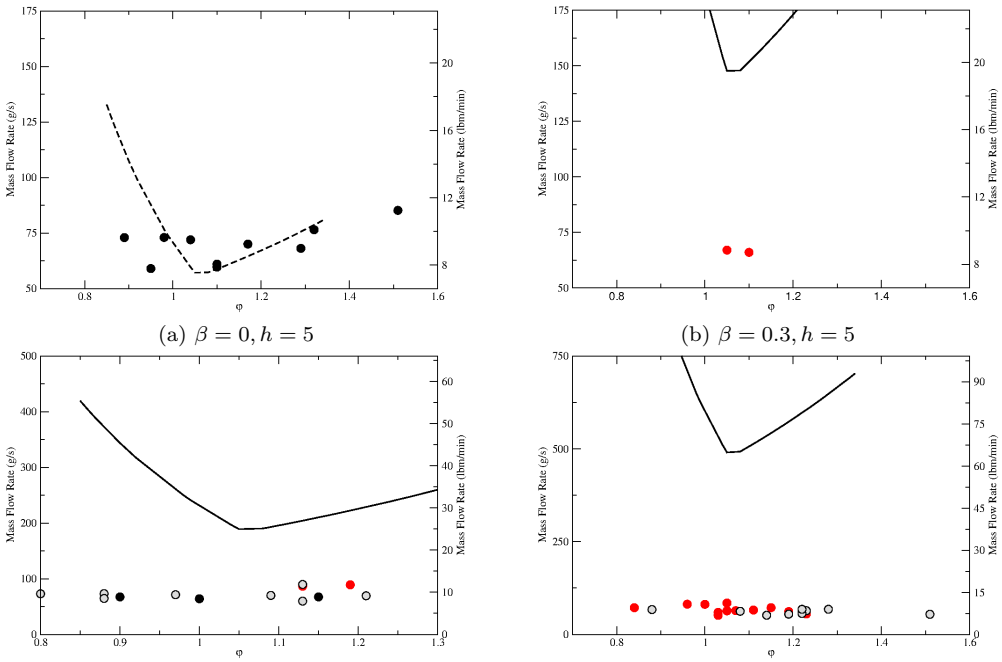

(a) $\beta = 0, h = 5$

(b) $\beta = 0.3, h = 5$

(c) $\beta = 0.3, h = 10$

(d) $\beta = 0.5, h = 10$

Figure 17: Model performance compared to other experimental engines at Poitiers, $h = 5$ mm (top row) and , $h = 10$ mm (bottom row) for nitrogen dilution ratios varying from $\beta = 0$ to $\beta = 0.5$. Black data points: successful 1 wave operation. Grey data points: 2 counter-rotating wave instability mode. Red data points: no detonation observed.

Chapter 5

Conclusion

A model to predict the lowest operable mass flow rate for an RDE was developed through the course of this work. This model captures the basic flow dynamics of the injection process as well as the detonation properties variations with respect to the injection state. The predicted mass flow rates compare very well to the experimental data for an RDE running on H_2+ enriched air collected in experiments performed by Russo [19]. The model also compares favourably to the $C_2H_4 + O_2 + N_2$ RDE tests run by Hansmetzger [20]. It is thought however that the scarcity of the detonation cell size data involving C_2H_4 based mixtures has contributed to the poor agreement between the experiments and model predictions at equivalence ratios that deviate greatly from the stoichiometric condition.

5.1 Future Work

An injection system was designed to deliver gaseous fuels and oxidizers to an RDE in a confined facility. A maximum delivery mass flow rate of $\dot{m} \approx 600$g/s was attained. A premixed and non-premixed RDE was designed, built and operated with stoichiometric $H_2 + O2$ and stoichiometric $C_2H_4 + O_2$ mixtures. The injection system designed has proven to be reliable in the preliminary experiments. Ignition and single cycle propagation were observed. Unfortunately, to date, no stable RDE operation has been observed.

There are currently a number of proposed augmentations to the analytical model developed for this Master's degree. The most important augmentation aims to eliminate the model's major weakness: the fact that the cell sizes are not directly measured from experiments. The extrapolated cell sizes used in the present model assume that the effect of initial pressure variations and equivalence ratio variations are linearly independent. Currently, only experiments can definitely provide the correct cell size measurements. It will be necessary to run a series of experiments to measure cell sizes for specific fuel mixtures relevant to RDE experiments.

The RDE's design will also be modified in the coming months. A final simple modification to the current engine has been proposed. These geometry changes involve doubling the annulus thickness to 5mm to remain more consistent with RDE designs that have been tested around the world. There is also a complete engine redesign in progress which would allow for a variable area injector.

A number of improvements to the testing facility are currently being developed. First, a more sophisticated control system is currently being developed. This control system would keep the original system's capabilities while also adding data acquisition functions, the ability to synchronize pressure and temperature data with the Raspberry Pi and high-speed camera, and would also be able to diagnose any kind of misfire. Second, a more accurate method of measuring mass flow rates will be necessary. This can be accomplished by measuring the change in weight of the two collector tanks with the use of load cells. Another method of calculating a mass flow rate would be by manufacturing a custom thermocouple attachment to measure the temperature of the fluid inside the lines. Third, there are plans to eventually measure the thrust produced by an RDE. To accomplish this, a proper thrust stand will need to be designed and built. Finally, a high energy igniter for use with the RDE should be designed to move away from using a non-electric pyrotechnic cable to ignite the engine. These improvements are currently under development partly by five separate undergraduate Capstone Engineering Design projects.

Bibliography

[1] P. Wolanski, "Detonative propulsion," *Proceedings of the Combustion Institute*, vol. 34, pp. 125–158, Jan. 2013.

[2] E. Wintenberger and J. E. Shepherd, "Thermodynamic Cycle Analysis for Propagating Detonations," *Journal of Propulsion and Power*, vol. 22, p. 4, June 2006.

[3] F. K. Lu and E. M. Braun, "Rotating Detonation Wave Propulsion: Experimental Challenges, Modeling, and Engine Concepts," *Journal of Propulsion and Power*, vol. 30, pp. 1125–1142, Sept. 2014.

[4] R. Zhou, D. Wu, and J. Wang, "Progress of continuously rotating detonation engines," *Chinese Journal of Aeronautics*, vol. 29, pp. 15–29, Feb. 2016.

[5] Y. Kudo, Y. Nagura, J. Kasahara, Y. Sasamoto, and A. Matsuo, "Oblique detonation waves stabilized in rectangular-cross-section bent tubes," *Proceedings of the Combustion Institute*, vol. 33, pp. 2319–2326, Jan. 2011.

[6] B. Voitsekhovskii, "Stationary detonation," *Doklady Akademii Nauk UzSSR*, vol. 129, no. 6, pp. 1254–1256, 1959.

[7] B. Voitsekhovskii, "Stationary spin detonation," *Soviet Journal of Applied Mechanics and Technical Physics*, no. 3, pp. 157–164, 1960.

[8] F. A. Bykovskii and V. V. Mitrofanov, "Detonation combustion of a gas mixture in a cylindrical chamber," *Combustion, Explosion, and Shock Waves*, vol. 16, no. 5, pp. 570–578, 1980.

[9] J. Nicholls and R. Cullen, "The Feasibility of a Rotating detonation Wave Rocket Motor," Technical Documentary Report RPL-TDR-64-113, Michigan University, Ann Arbor, Michigan, Apr. 1964.

[10] T. C. Adamson Jr and G. Olsson, "Performance Analysis of a Rotating Detonation Wave Rocket Engine," *Astronautica Acta*, vol. 13, no. 4/5, pp. 405–415, 1967.

[11] I.-W. Shen and T. C. Adamson Jr, "Theoretical analysis of rotating two phase detonation in a rocket motor," tech. rep., Michigan University, 1973.

[12] G. L. Schott, "Observations of the structure of spinning detonation," *The Physics of Fluids*, vol. 8, no. 5, pp. 850–865, 1965.

[13] F. A. Bykovskii, V. V. Mitrofanov, and E. F. Vedernikov, "Continuous detonation combustion of fuel-air mixtures," *Combustion, Explosion and Shock Waves*, vol. 33, no. 3, pp. 344–353, 1997.

[14] F. A. Bykovskii, S. A. Zhdan, and E. F. Vedernikov, "Continuous Spin Detonations," *Journal of Propulsion and Power*, vol. 22, pp. 1204–1216, Nov. 2006.

[15] K. Goto, R. Yokoo, J. Kim, A. Kawasaki, K. Matsuoka, J. Kasahara, A. Matsuo, I. Funaki, D. Nakata, M. Uchiumi, and H. Kawashima, "Propulsive performance of rotating detonation engines in $ch_4/o_2$and $c_2h_4/o_2$for flight experiment," in *Proceedings of the International Colloquium on the Dynamics of Explosions and Reactive Systems*, 2019.

[16] P. Wolanski, "Rotating detonation wave stability," in *Proceedings of the International Colloquium on the Dynamics of Explosions and Reactive Systems*, 2011.

[17] V. Anand, A. St. George, R. Driscoll, and E. Gutmark, "Characterization of instabilities in a Rotating Detonation Combustor," *International Journal of Hydrogen Energy*, vol. 40, pp. 16649–16659, Dec. 2015.

[18] S. J. Meyer, M. D. Polanka, F. Schauer, R. J. Anthony, C. A. Stevens, J. Hoke, and K. D. Rein, "Experimental characterization of heat transfer coefficients in a rotating detonation engine," *Proceedings of the 55th AIAA Aerospaces Sciences Meeting*, Jan. 2017.

[19] R. M. Russo, "Operational Characteristics of a Rotating Detonation Engine Using Hydrogen and Air," Master's thesis, Air Force Institute of Technology, 2011.

[20] S. Hansmetzger, *Etude des modes de rotation continue d'une détonation dans une chambre annulaire de section constante ou croissante*. PhD thesis, Poitiers University, July 2018.

[21] J. Kindracki, P. Wolański, and Z. Gut, "Experimental research on the rotating detonation in gaseous fuels–oxygen mixtures," *Shock Waves*, vol. 21, pp. 75–84, Apr. 2011.

[22] M. Kaneshige and J. E. Shepherd, "Detonation Database," Explosion Dynamics Laboratory Report FM97-8, California Institute of Technology, Pasadena, California, Sept. 1999.

[23] M. Radulescu and J. H. Lee, "The Failure Mechanism of Gaseous Detonations: Experiments in Porous Wall Tubes," *Combustion and Flame*, vol. 131, pp. 29–46, 2002.